

## Instability of solid-liquid interfaces in magnesia single crystals

Jung-Hae Choi\* and Doh-Yeon Kim

School of Materials Science and Engineering and Center for Microstructure Science of Materials, Seoul National University, Seoul 151-744, Korea

The instability of a solid-liquid interface (ISLI) on MgO single crystals with a CaMgSiO<sub>4</sub> liquid containing either CoO or NiO was investigated. As a result of a reaction with CoO-CaMgSiO<sub>4</sub>, a (Mg,Co)O solid solution layer with a uniform thickness developed at the surface of the MgO crystal. In contrast, when a MgO single crystal was reacted with NiO-CaMgSiO<sub>4</sub>, severe liquid penetration into the single crystal occurred, which resulted in a sponge-like structure. The results were examined in terms of the ISLI induced by the coherency strain energy, which were confirmed by conventional Transmission Electron Microscopy (TEM) observations, Convergent Beam Electron Diffraction (CBED) and Electron Probe Microanalysis (EPMA).

**Key words:** MgO single crystal, Diffusion, Solution-reprecipitation, Coherency strain energy, Instability of solid-liquid interface (ISLI)

### Introduction

When a liquid volume fraction in liquid-phase sintered materials is sufficiently high for solid grains to be separated, dissolution-and-reprecipitation has been observed to occur between the surface areas of a single grain, resulting in a corrugated solid-liquid interface [1-4]. This phenomenon, which is referred to as an instability of the solid liquid interface (ISLI), is known to occur when the compositional equilibrium between the grains and the liquid is broken by either changing the temperature or by introducing another element into the matrix.

This is interesting because the observed microstructural evolution does not coincide with the interfacial energy minimization. Recently, ISLI has been observed in various metallic and ceramic systems [1-4] and the diffusion coherency strain that develops in a thin solution zone has been experimentally determined to be the cause. It has been proposed that if a solution layer, which forms in the initial stages of the equilibration reaction, remained coherent with the parent crystalline lattice, coherency strain energy can develop. However, it was also reported that if the solution layer becomes thick, it loses its coherency with the production of misfit dislocations, which is referred to as coherency breaking [5]. Therefore, no further migration is expected to occur.

The aim of this study was to investigate the possible ISLI of an MgO single crystal and to elucidate the driving force of this instability. For this purpose, an

MgO single crystal was reacted with CaMgSiO<sub>4</sub> (hereafter, CaMgSiO<sub>4</sub> will be referred to as "CMS") liquid containing CoO and NiO, respectively.

### Experimental Procedure

MgO single crystals embedded in powder mixtures of 80CoO-20CMS and 80NiO-20CMS (wt%), respectively, were heat-treated at 1500°C. According to the pseudo-binary phase diagram of MgO-CMS [6], the liquid that appears at 1485°C is not soluble in MgO. On the other hand, both Co<sup>2+</sup> and Ni<sup>2+</sup> have the same valency as Mg<sup>2+</sup> and all of their oxides have an identical NaCl-type crystal structure. Therefore, CoO-MgO and NiO-MgO systems are known to form a complete solid solution without the formation of any new phases [7]. Although the phase diagrams of the NiO-CMS and CoO-CMS systems have not been reported, it is believed that both NiO and CoO are soluble in CMS because they are known to be highly soluble in silicate liquids [8]. Therefore, the composition of the MgO single crystal that is in contact with CoO-CMS and NiO-CMS, respectively, is expected to change during heat-treatment.

An MgO single crystal composed of {100} surfaces was cut into a rectangular shape (1 × 5 × 3 mm<sup>3</sup>). The surfaces were polished with a diamond paste down to 1 μm. Polishing oil and acetone were used to prevent hydration during the preparation of the MgO single crystal specimen [9]. In order to identify the initial position of the interface after heat-treatment, some of the MgO single crystals were pre-heat-treated at 1000 °C for 10 minutes after spreading a Pt paste (TR 7905, Tanaka Co., Japan) onto the {100} surfaces.

The CaMgSiO<sub>4</sub> powder was prepared from a mixture

\*Corresponding author:  
Tel : +82-2-880-8862  
Fax : +82-2-882-8164  
E-mail: choijh@plaza1.snu.ac.kr

of reagent-grade,  $\text{CaCO}_3$ ,  $\text{MgO}$  and  $\text{SiO}_2$  (all from Shinyo Pure Chemical Co., Japan). The powders were weighed and ball-milled for 24 h using a teflon-lined jar with ethanol and alumina balls. After drying, the powders were calcined at  $1400^\circ\text{C}$  for 2 h and ground to pass a 325-mesh sieve. The  $\text{MgO}$  powder was calcined at  $1200^\circ\text{C}$  for 1 h before use. The complete formation of CMS was confirmed by X-ray diffraction (XRD; DMAX-IIA, Rigaku, Japan). Powders of  $\text{CoO}$  (Kanto Chemical Co. Inc., Japan)-CMS and  $\text{NiO}$  (Wako Pure Chemical Industries LTD., Japan)-CMS were mixed for 1 h in an  $\text{Al}_2\text{O}_3$ -lined ball mill with ethanol, respectively. After drying, the powders were again milled for 1 h.

The  $\text{MgO}$  single crystals were embedded in the 20CoO-80CMS and 20NiO-80CMS powders, separately, and then compacted into a cylindrical shape of 10 mm in diameter. The compacts were pressed hydrostatically under 90 MPa pressure. After placing the compacts on Pt foil in a closed alumina crucible, the heat-treatment was carried out at  $1500^\circ\text{C}$  for 0 h and 2 h with the heating and cooling rates of  $10^\circ\text{C}\cdot\text{min}^{-1}$ . The heat-treatment for 0 h means that the specimens were cooled immediately after the sintering temperature was reached.

The heat-treated specimens were polished perpendicular to the  $\{100\}$  surfaces. The microstructural observations and composition analyses of the interfacial regions were performed using optical microscopy and electron probe microanalysis (EPMA; Superprobe 733, Jeol, Japan), transmission electron microscopy (TEM; Philips EM-430), convergent beam electron diffraction (CBED). For EPMA, the  $K_\alpha$  radiation for each element was monitored with the incident electron beam voltage of 15 kV and beam current of 10 nA, and a nominal beam size of approximately  $5\text{ }\mu\text{m}$  was used. The oxide standards of 99.9% purity  $\text{CoO}$  and  $\text{NiO}$  and ZAF correction were used and the precision of the quantitative compositional analysis is believed to be 0.01%. The TEM specimens were prepared carefully so as not to introduce dislocations by polishing. Mechanical polishing was performed down to a specimen thickness of about  $30\text{ }\mu\text{m}$  and then the surfaces were Ar ion milled from both sides to remove the damaged surface layer induced by mechanical polishing and to obtain electron transparency.

## Results and Discussion

### Optical Microscopic Observation

Figure 1(a) shows the morphology of the (100) plane of the  $\text{MgO}$  single crystal heat-treated in the 80CoO-20CMS powder mixture at  $1500^\circ\text{C}$  for 2 h. The upper part of the microstructure shows almost spherical grains dispersed in the CMS liquid matrix. The average composition of those grains was determined by EPMA to be  $(\text{Mg}_{0.28}\text{Co}_{0.72})\text{O}$ . The residual pores are believed to contain impermeable nitrogen gas trapped during the heat-treatment in air. The  $\text{MgO}$  single crystal at the

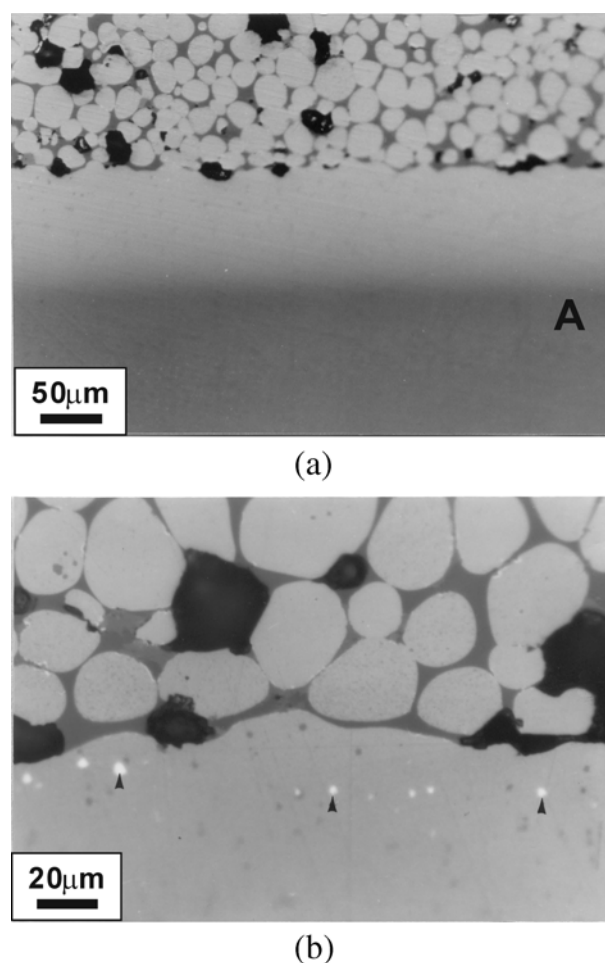


**Fig. 1.** (a) Microstructure of a  $\text{MgO}$  single crystal of a (100) plane heat-treated with a powder mixture of 80CoO-20CMS at  $1500^\circ\text{C}$  for 2 h. (b) Enlarged microstructure with the Pt markers, as indicated by the arrows.

lower part of the microstructure does not show any notable microstructural changes, except for the formation of a  $(\text{Mg},\text{Co})\text{O}$  solid solution layer of approximately  $100\text{ }\mu\text{m}$  thickness near the interface, which is distinct from the pure  $\text{MgO}$  crystal by its fainter color.

Figure 1(b) is the magnified microstructure under the same conditions used in Fig. 1(a) with the Pt markers. As indicated by the arrows, the Pt markers were observed in the interior of the  $\text{MgO}$  single crystal up to  $20\text{ }\mu\text{m}$  from the interface. This suggests that the spherical grains were dissolved in the liquid matrix and were reprecipitated on the  $\text{MgO}$  single crystal to form a solid solution layer. The  $(\text{Mg},\text{Co})\text{O}$  layer observed developed by two simultaneous processes; solution-reprecipitation and solid state diffusion.

The compositional analysis in Fig. 2 indicates that the  $\text{CoO}$  content is negligible at point A in Fig. 1(a), where it was predicted to be pure  $\text{MgO}$ . The concentration of the  $\text{CaO}$  and  $\text{SiO}_2$  detected were negligible even in the solid-solution region close to the liquid, (less than 0.01 mol%). The maximum  $\text{CoO}$  concentration in the  $(\text{Mg},\text{Co})\text{O}$  layer was 70 mol% at the interface

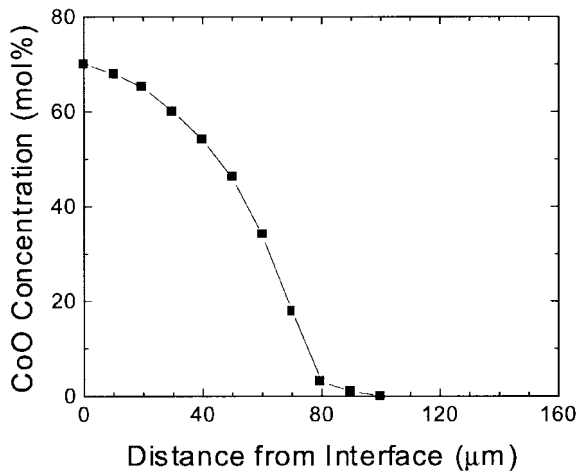


**Fig. 2.** Composition profile of CoO along the direction perpendicular to the (100) plane of the MgO single crystal heat treated at 1500°C for 2 h with a powder mixture of 80CoO-20CMS.

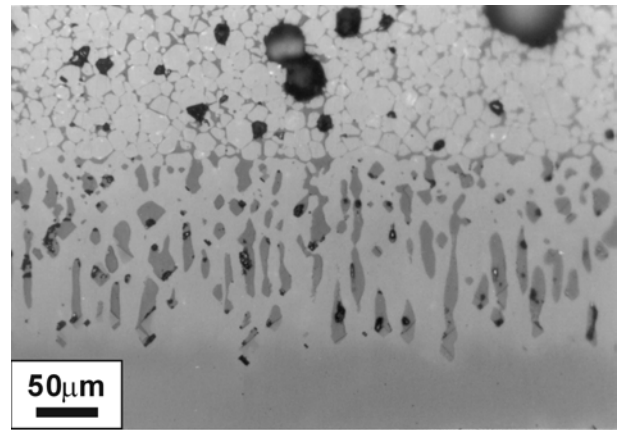
between the (Mg,Co)O layer and the liquid, and the CoO content decreased with increasing distance into the single crystal. On the other hand, the CoO concentration in the liquid phase was constant at approximately 30 mol%.

Figure 3(a) shows the (100) plane of the MgO single crystal embedded in the 80NiO-20CMS powder mixture and heat-treated at 1500°C for 2 h. The upper part of the figure shows a typical liquid-phase sintered microstructure, as already observed in the 80CoO-20CMS specimen. The sizes of the solid grains and residual pores are smaller and larger, respectively, compared to the CoO-CMS specimen. It appears that the rate of material transfer and consequently that of densification and grain growth in the NiO-CMS are slower than those in the CoO-CMS.

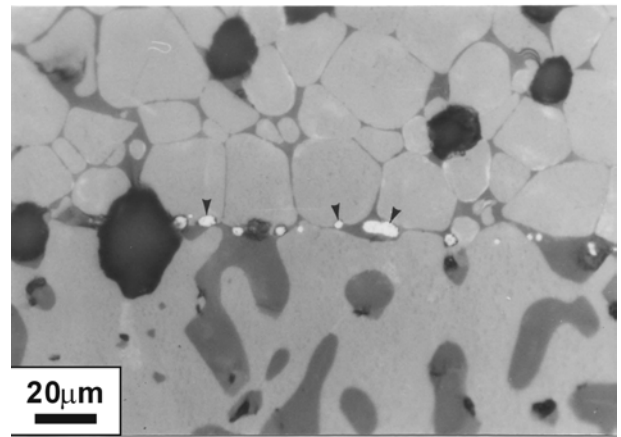
The most striking microstructural characteristics observed in Fig. 3 compared to Fig. 1 is the sponge-like structure that developed at the solid solution layer of the MgO single crystal up to approximately 160 μm. It was found that the liquid had penetrated severely into the single crystal, presumably along the <100> directions.

In Fig. 3(b), the Pt markers indicated by the arrows were observed at the boundary between the single crystal and the liquid. It is thus expected that the reprecipitation process of the (Mg,Ni)O solution on the MgO single crystal is negligible because the amount of the inward  $\text{Ni}^{2+}$  diffusion to the single crystal is almost the same as that of  $\text{Mg}^{2+}$  dissolution to the liquid in the convex region. This is consistent with the maximum concentration of NiO in the solid solution near the liquid phase, 50 mol%.

The NiO concentration profile determined in the reacted region of the MgO single crystal is shown in Fig. 4. The concentration gradient was relatively small up to approximately 80% of the total diffusion depth and then drastically decreased. The maximum NiO content in the solid-solution near the liquid phase was



(a)



(b)

**Fig. 3.** Microstructure of a MgO single crystal of a (100) plane heat-treated with a powder mixture of 80NiO-20CMS at 1500°C for 2 h. (b) Enlarged microstructure with the Pt markers, as indicated by the arrows.

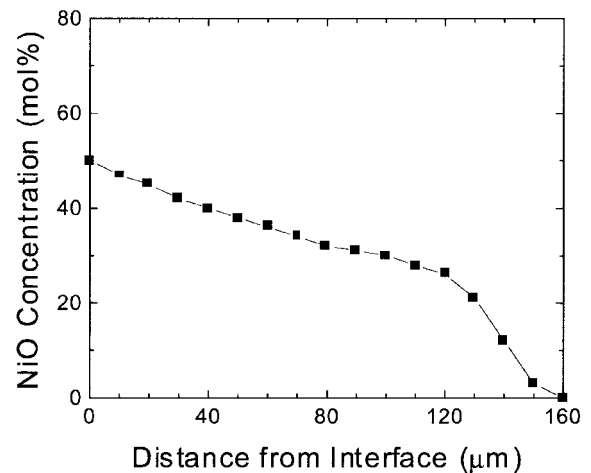


**Fig. 4.** Composition profile of NiO along the direction perpendicular to the (100) plane of the MgO single crystal heat treated at 1500°C for 2 h with a powder mixture of 80NiO-20CMS.

50 mol%. From the diffusion data reported by Wuensch and Vasilos [10] the diffusion coefficient of  $\text{Ni}^{2+}$  at 1500°C was calculated to be  $2.0 \times 10^{-11} \text{ cm}^2 \cdot \text{s}^{-1}$  and the thickness of the diffusion layer after heat-treatment for

2 h was expected to be around 4  $\mu\text{m}$ . Note that the real thickness of the sponge-like solution layer was approximately 160  $\mu\text{m}$ , which is 40 times larger than the calculated value. Composition analysis also showed that the liquid penetrating into the MgO crystal contained 43 mol% MgO and 12 mol% NiO. However, the liquid surrounding the (Mg,Ni)O spherical grains contained 24 mol% MgO and 35 mol% NiO. This indicates that  $\text{Ni}^{2+}$  entered the MgO single crystal, while  $\text{Mg}^{2+}$  left

through the liquid media.

### TEM Observations

Figure 5(a) shows a TEM bright field image of the convex single crystal region, heat-treated with 20NiO-80CMS at 1500°C for 0 h to observe the initial stages of ISLI. The electron beam direction is close to the  $\langle 111 \rangle$  direction of MgO. Characteristic hexagonal dislocation network images are clearly illustrated and the dislocations are aligned to form low angle grain boundaries. The boundary indicated by the arrow in Fig. 5(a) is an example of a low angle grain boundary, which is composed of a dislocation network. The same type of dislocation network was observed by Moriyoshi and Ikegami [11] in an annealed MgO single crystal, which had a large number of dislocations. It was expected that the dislocations were initially generated by lattice mismatch between the (Mg,Ni)O solid solution layer and the MgO, and formed dislocation networks - low angle grain boundaries- by a dislocation association and rearrangement during heat-treatment. Figure 5(b) shows a magnified image of the arrowed low angle grain boundary shown in Fig. 5(a).

The local lattice parameters of (Mg,Ni)O at both sides of the arrowed low angle grain boundary in Fig. 5(b) were compared by the CBED technique. Figure 5(c) shows the Zero Order Laue Zone (ZOLZ) discs in the exact  $[332]$  zone axis obtained from points A and B in Fig. 5(b). The Higher Order Laue Zone (HOLZ) line patterns observed in A and B are identical, which means that there are the same lattice parameters and consequently no Ni concentration difference across this low angle grain boundary. This suggests that the dislocation networks resulted from a slight misorientation between adjacent grains produced by a rearrangement of the initial misfit dislocations, and not from the lattice mismatch strain across the boundary. Note that the diffusion flux of  $\text{Ni}^{2+}$  is not unidirectional in the convex region of the crystal.

### Coherency Strain Energy

When a solid crystal is brought in contact with another liquid, its equilibration reaction occurs by two different processes; solution-reprecipitation, and lattice diffusion in the crystal. The interfacial reaction observed in the MgO single crystal with the CoO containing CMS liquid may be a typical example of such a normal equilibration reaction. However, the observed instability of solid-liquid interface for the MgO interface with the NiO-containing liquid can be explained in terms of another mechanism. A theoretical explanation that can justify the rapid reaction rate and unusual morphological changes should be introduced.

Recently, such an ISLI was also observed in Mo-Ni [1], TiC-Fe [2], TiC-Mo-Ni [3] and  $\text{ZrO}_2\text{-Y}_2\text{O}_3$  [4]. In these studies, it was suggested and experimentally proven that a diffusion coherency strain developed in

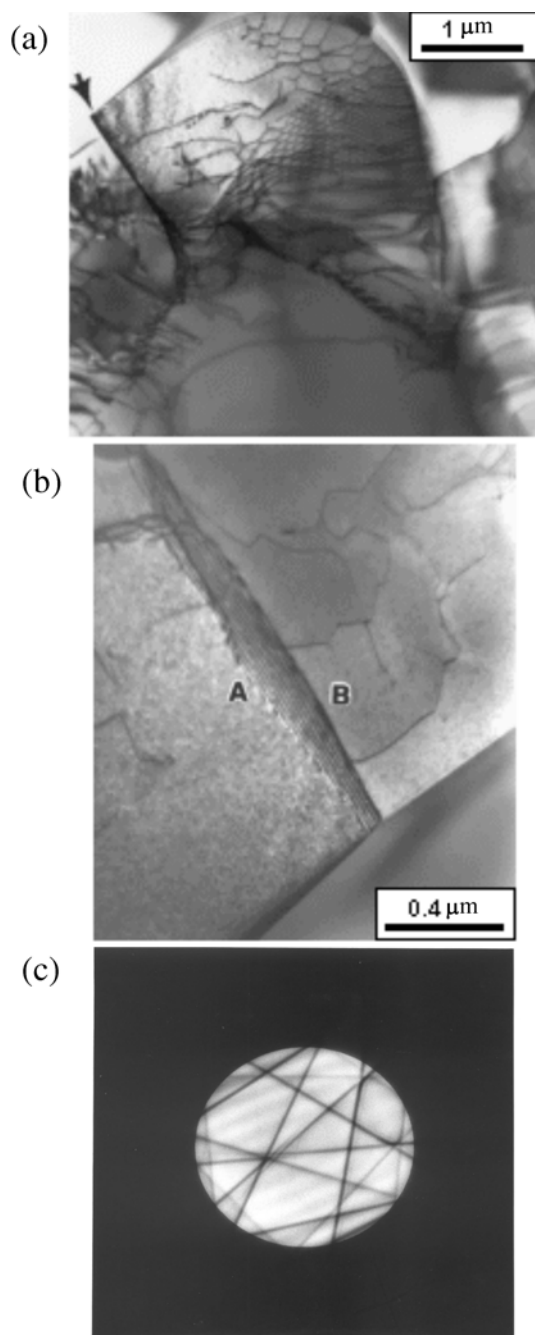


**Fig. 5.** (a) TEM bright field image of the solid solution region composed of low angle grain boundaries in the MgO single crystal of a (100) plane heat-treated with a powder mixture of 80NiO-20CMS at 1500°C for 0 h. (b) Enlarged TEM micrograph of the low angle grain boundary indicated by the arrow in Fig. 5(a). (c) HOLZ line pattern obtained from the regions A and B in Fig. 5(b).

the thin solution layer ahead of the dissolving concave interface induced ISLI. Sulonen [5] proposed earlier that if a solution layer that formed at the initial stage of the equilibration reaction remained coherent with the parent crystalline lattice, coherency strain energy, which is proportional to the orientation-dependent elastic modulus and the square of the elastic strain, can develop. In this case, the ratio of the solute diffusivity to the migration velocity of the interface,  $D/v$ , is known to be approximately the same as the thickness of the solution layer in the dissolving region.

However, if the solution layer becomes thick as a result of fast diffusion or time lapse, the coherency strain of the layer will be relaxed with the production of misfit dislocations to minimize the energy. In this situation, the total misfit can be shared by both elastic and plastic strain with the partitioning depending on the thickness of the solution layer [12]. Therefore, the energy of the misfit dislocations can be produced as a result of such coherency breaking. Once the coherency breaking occurs, the solution layer loses its coherency and no further migration is expected.

The interfacial characteristics of the MgO crystal observed during heat-treatment with CoO-CMS and NiO-CMS, respectively, were examined to evaluate the role of coherency strain energy in ISLI. The lattice parameters of the NaCl-type structure MgO, CoO and NiO are 0.421 nm, 0.426 nm and 0.418 nm, respectively [13]. In this respect, compressive and tensile stresses will develop in a thin solution layer of (Mg,Co)O and (Mg,Ni)O formed on MgO, respectively. For the (Mg,Ni)O layer that develops on a {100} plane of MgO, the  $D/v$  ratio was determined to be 96 nm. Since this  $D/v$  value is considerably larger than the lattice parameter of MgO, a solution layer, which may be coherent with the parent MgO lattice should exist in front of the dissolving solid interface, and its coherency strain energy can result in an ISLI. For the most chemically induced interface migration (CIIM) experimentally observed,  $D/v$  values between  $\sim 10$  and  $\sim 100$  nm are commonly reported [14,15], and such a substantial  $D/v$  value is generally regarded as an essential condition for either ISLI or CIIM.

Blendell *et al.* [15] reported the CIIM in liquid phase-sintered MgO by using CoO as a solute source at 1250°C. Note that the heat-treatment temperature is 250°C lower than that in the current experiments. The observed migration velocity of interface,  $v$ , was  $8.3 \times 10^{-7} \text{ cm}\cdot\text{s}^{-1}$  and the estimated  $D/v$  ratio was 110 nm by substituting the diffusivity at this temperature ( $9.1 \times 10^{-12} \text{ cm}^2\cdot\text{s}^{-1}$  [10]). Note that a similar value of 96 nm was obtained for the (Mg,Ni)O solution layer on the MgO {100} plane in these experiment. In this regard, the absence of an ISLI for the (Mg,Co)O solution layer in these experiment appears to be a consequence of the high diffusivity of  $\text{Co}^{2+}$  in MgO. At the heat-treatment temperature, 1500°C, coherency breaking is expected to

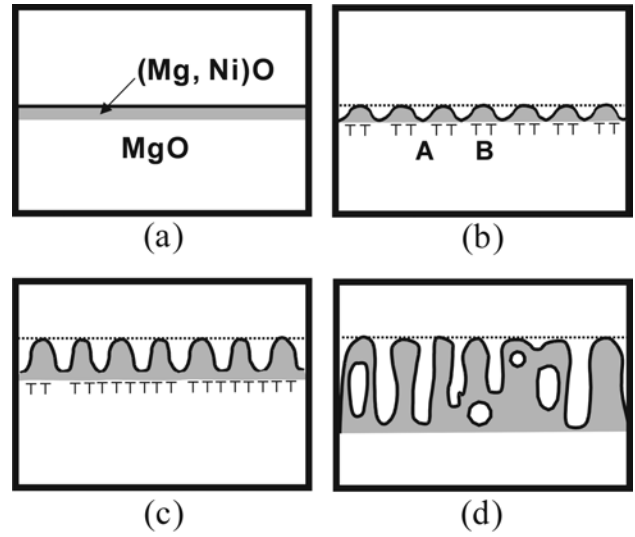


**Fig. 6.** Schematic evolution of the (100) surface of a MgO single crystal embedded in a powder mixture of 80NiO-20CMS. The broken lines indicate the initial position of the interface.

occur very easily because of the large  $D/v$  ratio of the (Mg,Co)O solution layer.

Figure 6 shows the schematic evolution of the ISLI on the (100) surface of the MgO single crystal embedded in NiO-CMS. The thin diffusion layer (Fig. 6(a)) formed by  $\text{Ni}^{2+}$  diffusion into an initially planar surface is expected to induce local coherency breaking, as suggested by Matthews *et al.* [12] (Fig. 6(b)). Consequently, a wave-like interface develops by the local dissolution of a high-energy interfacial region (indicated by A) where the coherency is maintained. Since MgO and NiO are highly soluble in the liquid matrix [6, 8], materials dissolved from region A are expected to diffuse into the liquid or reprecipitate on region B where the coherency has been broken. The Pt marker experiments suggest that the dissolved  $\text{Mg}^{2+}$  diffuses into the liquid phase as a result of its high solubility. Note that the (Mg,Ni)O in region A is in a higher energy state than that in region B due to coherency strain. However, in the dissolved region A the dissolution rate is expected to decrease with increasing curvature. The consequent decrease in interfacial migration velocity,  $v$ , may give rise to a thick diffusion layer, which is equal to  $D/v$ . Thus, coherency breaking is also believed to occur in some dissolved regions, as illustrated in Fig. 6(c).

The classical ISLI theory can be applied to the early stages of the formation of the wave boundary. Although it has not been studied sufficiently to draw any definitive conclusions, the interface energy and cleavage characteristics of the MgO crystal are also predicted to affect the further preferential penetration of the liquid. Once the misfit dislocations spread all over the solid solution layer, cleavage is expected to occur at a relatively low strain on the {100} planes [16], which may accelerate liquid penetration into the single crystal (Fig. 6(d)).

This is because the equilibrium shape of the MgO single crystal in air is a cube composed of a {100} plane group.

### Conclusions

The solid-liquid interfacial reaction of a MgO single crystal with CMS liquid containing either CoO or NiO was investigated. As a result of a reaction with CoO-CMS, a uniform layer of a (Mg,Co)O solid solution developed on the surface of the MgO crystal. In contrast, when the MgO single crystal was reacted with NiO-CMS, instability of solid-liquid interface (ISLI) was observed. The (Mg,Ni)O solid solution that formed at the surface of the MgO single crystal exhibited a sponge-like microstructure. Severe liquid penetration into the single crystal resulted in a large increase in the solid-liquid interfacial area.

The interfacial phenomena observed during the formation of (Mg,Co)O was explained in terms of a simple solution-reprecipitation and lattice diffusion process. On the other hand, the ISLI during the (Mg,Ni)O formation was assumed to arise mainly from the coherency strain induced by  $\text{Ni}^{2+}$  diffusion into the MgO single crystal.

### Acknowledgment

The work is supported by the Creative Research Initiatives of the Korean Ministry of Science and Technology.

### References

1. W.H. Rhee and D.N. Yoon, *Acta Metall.* 35 (1987) 1447-51.
2. K.-W. Chae, D.-I. Chun, D.-Y. Kim, Y.J. Baik and K.Y. Eun, *J. Am. Ceram. Soc.* 73[7] (1990) 1979-1982.
3. D.-I. Chun, K.-Y. Eun and D.-Y. Kim, *J. Am. Ceram. Soc.* 76[8] (1993) 2049-2052.
4. J.W. Jeong, D.N. Yoon and D.-Y. Kim, *Acta Metall. Mater.* 39[6] (1991) 1275-79.
5. M.S. Sulonen, *Acta Metall.* 8[10] (1960) 669-676.
6. R.M. El-Shahat and J. White, *Trans. Brit. Ceram. Soc.* 65 (1966) 309.
7. Fig. 51 and 258 in "*Phase Diagrams for Ceramists*" (The Am. Ceram. Soc., 1969).
8. See, for example Fig. 4245, 4517, 4555 and 5382 in "*Phase Diagrams for Ceramists*" (The Am. Ceram. Soc., 1969).
9. M.P. Delplancke-Ogletree, M. Ye, R. Winand, J.F. De Marneffe and R. Deltour, *J. Mater. Res.* 14[5] (1999) 2133-2137.
10. B.J. Wuensch and T. Vasilos, *J. Chem. Phys.* 36[11] (1962) 1017-1022.
11. Y. Moriyoshi and T. Ikegami, in "*Advances in Ceramic, Vol.10, Structure and Properties of MgO and  $\text{Al}_2\text{O}_3$  Ceramics*" (The Am. Ceram. Soc., 1984) p. 258.
12. J.W. Matthews, D.C. Jackson and A. Chambers, *Thin Solid Films* 26 (1975) 129-134.
13. R.C. Weast, in "*Handbook of Chemistry and Physics, 70ed.*" (CRC Press, 1989) p. B-193.
14. J.W. Jeong, D.N. Yoon and D.-Y. Kim, *J. Am. Ceram. Soc.* 73[7] (1990) 2063-2067.
15. J.E. Blendell, C.A. Handwerker, C.A. Shen and N.D. Dang, in "*Ceramic Microstructures '86, Role of Interface*" (Plenum Press, 1986) p. 541.
16. R.W. Davidge, in "*Mechanical Behavior of Ceramics*" (Cambridge University Press, 1979) p. 54, 77.